Materials Engineering and Technologies

https://met.cultechpub.com/met

Cultech Publishing

Article

Synthesis and Characterization of Biogenic Silver Nanoparticles Using Vernonia anthelmintica Extract and Their Biological Activities

Rehana Bibi[1], Nasihat[2], Najmaldin Ezaldin Hassan[3,*]

[1]Department of Chemistry, Women University of Swabi, Swabi, Khyber Pakhtunkhwa, Pakistan

[2]School of Chemistry and Chemical Engineering, Hainan Normal University, Hainan, China

[3]College of Engineering, Civil and Environment Department, University of Zakho, Kurdistan Region, Iraq

[*]Corresponding author: Najmaldin Ezaldin Hassan, Hassanezaldin23@gmail.com

Abstract

The biosynthesis of silver nanoparticles (AgNPs) using biological methods has gained increasing attention due to their broad range of applications. In this study, AgNPs were synthesized via a simple and eco-friendly approach using *Vernonia anthelmintica* stem and leaf extract as both a reducing and stabilizing agent. The synthesized nanoparticles were characterized through UV-Visible spectroscopy, Fourier-transform infrared spectroscopy (FTIR), scanning electron microscopy (SEM), energy-dispersive X-ray spectroscopy (EDX), and X-ray diffraction (XRD). UV-Vis analysis revealed a distinct surface plasmon resonance (SPR) peak at 413 nm, confirming the formation of AgNPs. XRD results indicated a crystalline structure with an average crystallite size of approximately 49 nm, while SEM analysis revealed an average particle size of around 21 nm, suggesting polydispersity. EDX spectra confirmed the presence of elemental silver, and FTIR analysis identified functional groups such as alkenes, dicarboxylic amino acids, and sulfonyl chlorides, indicating their role in the reduction and stabilization of the nanoparticles. The synthesized AgNPs exhibited notable antibacterial activity against *Staphylococcus aureus* (Gram-positive) and *Citrobacter* (Gram-negative), with inhibition zones of 20 mm and 18 mm, respectively. In contrast, the plant extract alone showed no antibacterial effect. The AgNPs also demonstrated antifungal activity against Echromonium, Penicillium, and Pythium, whereas the crude extract was inactive against these fungi. Additionally, antioxidant activity, assessed using the 2,2-diphenyl-1-picrylhydrazyl (DPPH) assay, showed significant radical scavenging potential by the extract.

Keywords

Green synthesis, Silver nanoparticles (AgNPs), *Vernonia anthelmintica*, Nanobiotechnology, Antimicrobial activity

Article History

Received: 05 June 2025 | Revised: 03 July 2025

Accepted: 14 July 2025 | Available Online: 18 July 2025

1. Introduction

The term "nano" is derived from the Greek word nanos, meaning "dwarf," and has become increasingly prevalent in modern scientific literature [1]. It is now widely used across disciplines, giving rise to terms such as nanometer, nanoscale, nanoscience, nanotechnology, and nanostructures [2]. Nanotechnology refers to the science and manipulation of matter at the scale of one billionth of a meter, involving the design, synthesis, and application of materials at the atomic and molecular level [3]. One of the central aspects of nanotechnology is the production of nanoparticles with controlled size, shape, composition, and functionality, which opens up numerous possibilities for technological innovation [4].

Nanotechnology research and development has expanded rapidly in the 21st century, especially in the synthesis of nanoparticles with dimensions typically below 100 nanometers [5-7]. Nanoparticles exhibit unique and often enhanced properties compared to their bulk counterparts, including increased surface area, catalytic reactivity, and improved antimicrobial activity [8,9]. These properties arise from their high surface-to-volume ratio, which enhances their interaction with biological and chemical environments [10].

Among the various types of nanoparticles, noble metal nanoparticles, especially silver nanoparticles (AgNPs), have attracted significant interest due to their remarkable physicochemical and biological properties [11]. AgNPs are known for their electrical conductivity, chemical stability, catalytic potential, and strong antimicrobial activity. Studies have shown that AgNPs often outperform other metal nanoparticles such as gold, copper, and palladium in biological applications [12-15].

AgNPs can be synthesized through physical, chemical, or biological (green) methods [16]. While conventional physical and chemical methods such as laser ablation, pyrolysis, vapor deposition, and sol-gel processes are effective, they often involve toxic solvents, high energy inputs, and generate hazardous by-products [17]. In contrast, green synthesis offers an eco-friendly, cost-effective, and scalable alternative that avoids the use of harmful chemicals [18]. Green synthesis typically utilizes plant extracts, fruits, or microorganisms as natural reducing and stabilizing agents [19]. This method not only supports sustainable chemistry but also enhances the biocompatibility and biological efficacy of the resulting nanoparticles [20].

The success of green synthesis depends on multiple factors, including the choice of plant extract, the concentration of reactants, pH, temperature, and reaction time [21]. Various plant parts such as leaves, stems, seeds, and peels have been successfully used to synthesize AgNPs with diverse shapes (spherical, rod-shaped, triangular, etc.) and sizes ranging between 1 and 100 nm [22]. For example, extracts from tamarind, onion, basil, and banana peels have demonstrated effective synthesis of silver and gold nanoparticles with promising applications [23].

In this context, *Vernonia anthelmintica* (also known as Centratherum anthelminticum), commonly referred to as Blue Fleabane emerges as a valuable candidate for green synthesis [24]. This herbaceous plant, belonging to the family Asteraceae (Compositae), is native to South Asia and widely used in traditional medicine [25]. It grows up to 60-90 cm in height and is characterized by pubescent stems and dark brown oily seeds [26]. In folk medicine, *V. anthelmintica* has been used to treat a wide range of ailments including malaria, fever, worm infestations, inflammation, infections, cancer, and gastrointestinal disorders [26]. The seeds are also traditionally used as blood purifiers and remedies for diabetes, toothache, and dysentery [27].

Given the therapeutic potential of *V. anthelmintica*, its use as a reducing and stabilizing agent for the green synthesis of silver nanoparticles presents an exciting opportunity. The aim of this study is to synthesize AgNPs using stem and leaf extracts of *V. anthelmintica*, characterize the synthesized nanoparticles using various analytical techniques, and evaluate their antibacterial, antifungal, and antioxidant properties.

2. Materials and Methods

2.1 Chemicals

Silver nitrate ($AgNO_3$) was procured from E. Merck (D-6100 Darmstadt, F.R. Germany). Nutrient agar, Mueller-Hinton broth, and Mueller-Hinton agar used for bacterial culture and antimicrobial testing were obtained from Merck, Pakistan. Other materials used in this study included plant extracts, fungal strains, Petri plates, agar media, synthesized AgNPs, dimethyl sulfoxide (DMSO), an incubator, micropipettes, screw-cap test tubes, an autoclave, Potato Dextrose Agar (PDA), a magnetic stirrer, and standard antifungal agents (Miconazole and Amphotericin B). The antioxidant assay utilized 2,2-diphenyl-1-picrylhydrazyl (DPPH).

2.2 Collection and Preservation

Fresh aerial parts of *V. anthelmintica* at the leafy stage were collected from Shanghai, China. The collected plant material was thoroughly cleaned, washed with tap water, and shade-dried. Once completely dried, the specimens were ground into a fine powder using an electric grinder.

2.3 Preparation of Extract

The aerial parts of *V. anthelmintica* were ground using an electric grinder to obtain a fine powder with a 60-mesh particle size. A 500 g portion of the powdered sample was soaked in 1.5 L of 70% methanol for 15 days at room temperature. After maceration, the extract was filtered using Whatman filter paper No. 1823. The filtrate was then concentrated using a rotary evaporator at 40°C and stored at 4°C for subsequent use in silver nanoparticle synthesis.

2.4 Preparation of Silver Nitrate Solution

All glassware used in the synthesis process was initially cleaned with aqua regia (a 3:1 mixture of hydrochloric acid and nitric acid) to remove any potential metal contaminants. Afterward, the glassware was thoroughly rinsed with distilled water and dried before use to ensure a contamination-free environment. A 1 mM $AgNO_3$ stock solution was prepared by accurately weighing 0.016986 g of $AgNO_3$ and dissolving it in a small volume of deionized water. The solution was then transferred to a 100 mL volumetric flask and the volume was made up to the mark with deionized water. The solution was mixed thoroughly and stored in a dark amber bottle to prevent photodegradation until further use in the biosynthesis of silver nanoparticles.

2.5 Preparation of Extract Solution

To prepare the plant extract solution, 0.5 g of the dried methanolic extract of *V. anthelmintica* was accurately weighed using an analytical balance. The weighed extract was first dissolved in a small quantity of deionized water under continuous stirring to ensure complete solubilization. The solution was then transferred to a 100 mL volumetric flask, and the volume was made up to the mark with deionized water. The mixture was thoroughly shaken to ensure uniform dispersion. The final extract solution was stored at 4°C in a sterile, amber-colored container to prevent degradation and contamination before its use in the biosynthesis of silver nanoparticles.

2.6 Synthesis of Silver Nanoparticles

The biosynthesis of AgNPs was carried out by mixing the prepared *V. anthelmintica* extract solution with a 1 mM aqueous solution of $AgNO_3$ in various volume ratios (1:2, 1:4, 1:6, and 1:8). For each reaction, the plant extract was added dropwise into the silver nitrate solution under constant magnetic stirring to ensure uniform mixing and effective interaction between the phytochemicals and silver ions. The reaction mixtures were stirred continuously at room temperature for a period of 4 hours. A gradual color change from pale yellow to dark brown was observed during the course of the reaction, indicating the formation of silver nanoparticles. This visible color transformation is attributed to the excitation of Surface Plasmon Resonance (SPR), which serves as the primary and preliminary confirmation of nanoparticle synthesis. The reaction mixtures were further monitored and stored for subsequent characterization.

3. Results and Discussion

3.1 Synthesis of Silver Nanoparticles

This study focuses on the environmentally friendly biosynthesis of AgNPs using the aerial part extract of *V. anthelmintica* as both a reducing and capping agent. The biosynthesis process involves mixing the plant extract with a 1 mM $AgNO_3$ solution in various volume ratios. The reaction mixture was kept under continuous magnetic stirring to ensure proper interaction between the plant extract and the silver ions. As the reaction progressed, a visible color change from pale yellow to brown occurred, which marks the initial formation of silver nanoparticles. This color shift is attributed to the phenomenon known as SPR [28]. When electromagnetic radiation falls on the surface of metal nanoparticles, it induces oscillation of free electrons at the surface, particularly when the size of the nanoparticle is below 60 nm. The energy absorbed during this oscillation leads to the distinctive color change, providing a clear indication of nanoparticle formation [29]. The biomolecules present in the Vernonia anthelmintica aerial extract play a crucial role in stabilizing and reducing the silver ions (Ag^+) to their metallic form (Ag^0) [22]. These biomolecules cap the surface of the AgNPs, preventing their aggregation and helping control their size. The synthesized AgNPs exhibit a characteristic absorbance peak in the range of 400-500 nm, which is typically associated with the SPR of AgNPs [22].

3.2 Optimization of Silver/Extract Ratio for Silver Nanoparticles

To optimize the synthesis of AgNPs and identify the optimal ratio of plant extract to silver nitrate solution that yields the maximum absorbance, various ratios were tested. The ratios examined were 1:2, 1:4, 1:6, and 1:8 (plant extract to silver nitrate solution, by volume) (Figure 1). These ratios were chosen to evaluate the impact of different extract concentrations on the synthesis process and the properties of the resulting AgNPs. All ratios produced an absorbance peak within the typical range of 400-500 nm, which is characteristic of the SPR of AgNPs. The SPR peak in this range is a clear indication of nanoparticle formation and is commonly observed in AgNPs due to their strong interaction with light [30,31]. Among the tested ratios, the 1:2 ratio of plant extract to silver nitrate solution exhibited the sharpest and most prominent SPR peak, demonstrating the highest absorbance. This suggests that the 1:2 ratio is the most effective for synthesizing silver nanoparticles with optimal size and stability. At this ratio, the silver ions were more efficiently reduced by the plant extract, leading to the formation of nanoparticles with enhanced optical properties. The results of this optimization study highlight that while all ratios successfully generated AgNPs, the 1:2 ratio provides the best conditions for maximizing the synthesis of AgNPs with improved characteristics. This optimized ratio will be used in subsequent experiments for further analysis of the nanoparticles' properties and their potential applications.

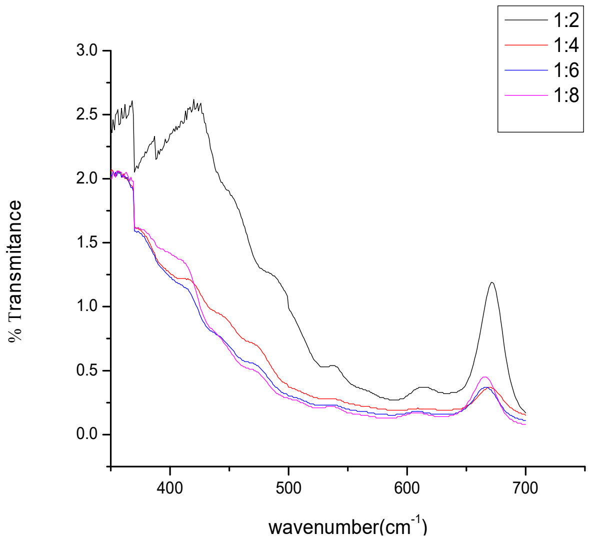

Figure 1. Absorbance at different ratio of Silver and Extract solution.

3.3 Optimization of Time for Silver Nanoparticles

UV-Vis spectroscopy is a crucial technique for characterizing metal nanoparticles, as it allows for the identification of the Surface SPR peak, which is a result of the collective oscillation of free electrons on the metal nanoparticle's surface (Figure 2). These free electrons resonate with incident light waves, producing a characteristic absorption band, typically observed in the range of 400-500 nm for AgNPs. The formation of AgNPs was visually confirmed after mixing the *V. anthelmintica* aerial part extract with the silver nitrate solution. A noticeable change in the color of the solution, from pale yellow to dark brown, served as the initial indication of AgNPs formation. To further confirm the formation of nanoparticles and to optimize the reaction time, UV-Vis spectroscopy was employed. The same ratio of plant extract to silver solution was stirred for varying time intervals, ranging from 15 minutes to 195 minutes, in increments of 15 minutes (i.e., 15, 30, 45, 60, 75, 90, 105, 120, 135, 150, 165, 180, and 195 minutes) (Figure 2). The UV-Vis spectral data revealed that significant nanoparticle formation occurred after 165 minutes of reaction, as evidenced by the appearance of a distinct SPR peak at 413 nm (Figure 2). This broad absorption spectrum indicated the formation of larger-sized nanoparticles, which corresponds with the typical behavior of AgNPs as the reaction progresses. The SPR peak observed at 413 nm is consistent with results reported in previous studies. For example, Rao et al. [32] synthesized AgNPs from Couroupita guianensis leaf extract, observing a SPR peak in the range of 415-425 nm. Similarly, Saikia et al. [33] synthesized AgNPs from Couroupita guianensis flower petal extract, which exhibited a SPR peak at 418-424 nm. The consistency of these findings with our own UV-Vis results, showing a peak at 413 nm, strongly suggests that the silver nanoparticles synthesized using *V. anthelmintica* extract exhibit properties similar to those of silver nanoparticles synthesized using other plant extracts. This further supports the effectiveness of *V. anthelmintica* as a reducing and stabilizing agent in the green synthesis of AgNPs.

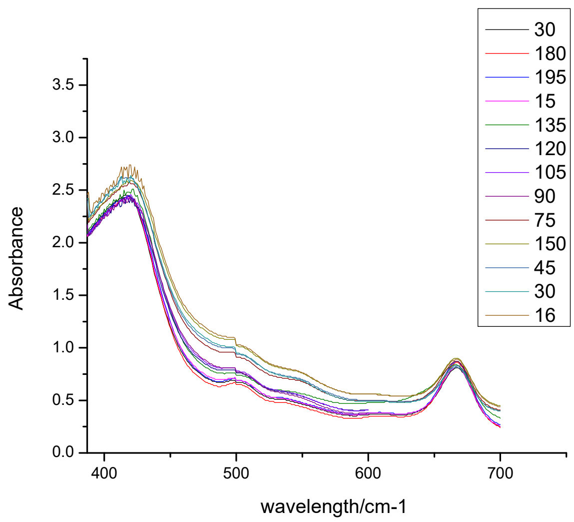

Figure 2. Time (min) Optimization of AgNPs of leaf and stem extract.

3.4 X-Rays Diffration Analysis (XRD)

X-ray Diffraction (XRD) analysis was employed to investigate the crystalline nature of the synthesized AgNPs. The XRD patterns presented in Table 1. provide evidence of the formation of silver nanoparticles using the aerial part of *V. anthelmintica*. The XRD spectra revealed several size-dependent features, including variations in peak position, height, and width, which are indicative of the formation of nanoparticles with different sizes and crystalline structures. Upon the complete reduction of silver ions (Ag^{+}) to metallic silver (Ag^{0}), several Bragg reflections were observed in the XRD pattern. These reflections can be indexed based on the cubic crystal structure of silver (Ag^{0}), with diffraction peaks at 2θ values of 27.95° (151), 32.35° (156), and 46.30° (107), which are consistent with those reported for standard silver metal (Ag^{0}) [80]. These peaks confirm that the synthesized silver nanoparticles are crystalline in nature. The most intense diffraction peak was observed at 32.35° (156), indicating a dominant crystallographic plane in the nanoparticles. This high intensity suggests a well-ordered arrangement of silver atoms within the nanoparticle structure. The average particle size of the silver nanoparticles was calculated using the Debye-Scherrer equation, based on the width of the (156) Bragg reflection. The calculated particle size was approximately 49 nm, which is consistent with the typical range of silver nanoparticles synthesized via green synthesis methods. These results align with earlier studies. For example, Ramesh et al. [34] synthesized silver nanoparticles using the leaf extracts of Ocimum tenuiflorum (AgNP1) and Catharanthus roseus (AgNP2). In their study, AgNP1 exhibited three distinct diffraction peaks at 27.1°, 32.2°, and 46.2°, corresponding to the (226), (264), and (200) planes of the cubic face-centered silver structure (Table 1). In contrast, AgNP2 showed four peaks at 27.1°, 32°, 39.2°, and 44.8°, indexed to the reflection planes (226), (264), (111), and (200) of silver. These findings are consistent with the results of the XRD analysis of *V. anthelmintica*-derived AgNPs, further confirming that the nanoparticles synthesized in this study exhibit characteristics similar to those observed in other plant-based green synthesis methods.

Table 1. XRD analysis of AgNPs of *V. anthelmenthica.*

S.No	2θ (degree)	FWHM (degrees)	β = FWHM × (π / 180)	D = k λ / $\beta^{1/2}$. Cos θ (nm)
1	27.95	28.00	0.00819	38nm
2	32.35	35.25	0.00610	53nm
3	46.30	46.11	0.00706	56nm

3.5 Scanning Electron Microscopy (SEM)

The size and morphology of the synthesized AgNPs were investigated using Scanning Electron Microscopy (SEM) (Figure 3). The SEM images revealed that the AgNPs exhibited a spherical shape and were uniform in size. The average particle size was calculated to be approximately 21 nm, as shown in Figure 3. This finding is consistent with the typical morphology of silver nanoparticles synthesized through green synthesis methods. Similar results have been reported in earlier studies. For example, Rajasekar et al. [35] used plant extracts of Azadirachta indica, Tridax procumbens, and Aegle marmelos for silver nanoparticle synthesis, and their SEM images showed spherical nanoparticles with sizes ranging from 35 to 65 nm, well-distributed without aggregation [7,8]. Similarly, Gavade et al. [36] synthesized AgNPs using Averrhoa carambola fruit extract, and their SEM analysis revealed uniform nanoparticles with sizes ranging from 40 to 50 nm. In conclusion, the SEM analysis of the synthesized AgNPs in this study is in agreement with the findings of previous research, confirming that the *V. anthelmintica*-synthesized AgNPs exhibit uniform spherical morphology with a particle size of around 21 nm. In addition to morphological evaluation, SEM analysis supports the understanding of the structure-property relationships of the AgNPs. The smooth, compact surface and uniform size suggest good adhesion potential when interacting with bacterial membranes or embedding within composite materials. The absence of cracks or fractured particles further indicates strong structural stability, reducing the chances of breakage or pull-out during application. These features are essential for maintaining the functional performance of the AgNPs, particularly in biomedical or environmental systems where mechanical and surface integrity are critical.

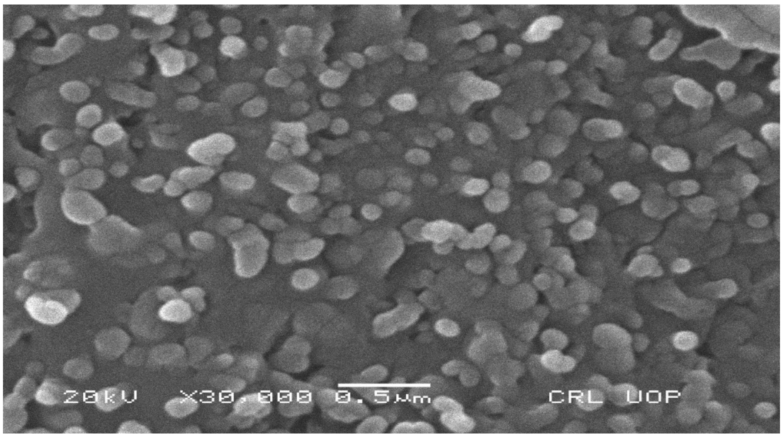

Figure 3. SEM analysis of silver nanoparticles of *V. anthelmintica.*

3.6 Energy Dispersive X-ray Analysis

The Energy Dispersive X-ray (EDX) analysis of the synthesized AgNPs provides valuable insights into the elemental composition of the particles (Figure 4). The EDX spectrum of the silver nanoparticles exhibited a strong signal for silver (Ag) atoms, confirming the presence of pure silver at the 2.5 KeV energy level, which corresponds to the Surface Plasmon Resonance (SPR) band, as shown in Figure 4. This characteristic signal is a clear indicator of silver nanoparticles' successful synthesis. The EDX spectrum also revealed the presence of chlorine (Cl) and silicon (Si), which can be attributed to the plant extract used in the synthesis process. Furthermore, the signals for carbon (C), fluorine (F), and oxygen (O) in the spectrum suggest that biomolecules from the *V. anthelmintica* aerial part extract are bound to the surface of the AgNPs. These biomolecules likely act as stabilizing agents, preventing the nanoparticles from aggregation and enhancing their bioactivity.The EDX analysis strongly supports the conclusion that AgNPs were successfully synthesized using the aerial part extract of *V. anthelmintica* in this study. Similar results have been reported in previous studies. For example, Kotakadi et al. [37] utilized Abutilon indicum leaf extract for the biogenic synthesis of silver nanoparticles, and their EDX analysis also showed a strong silver signal. These findings are consistent with the results obtained in this study, confirming that the EDX analysis of the AgNPs synthesized from the aerial part extract of *V. anthelmintica* aligns with previous research on plant-mediated synthesis of AgNPs.

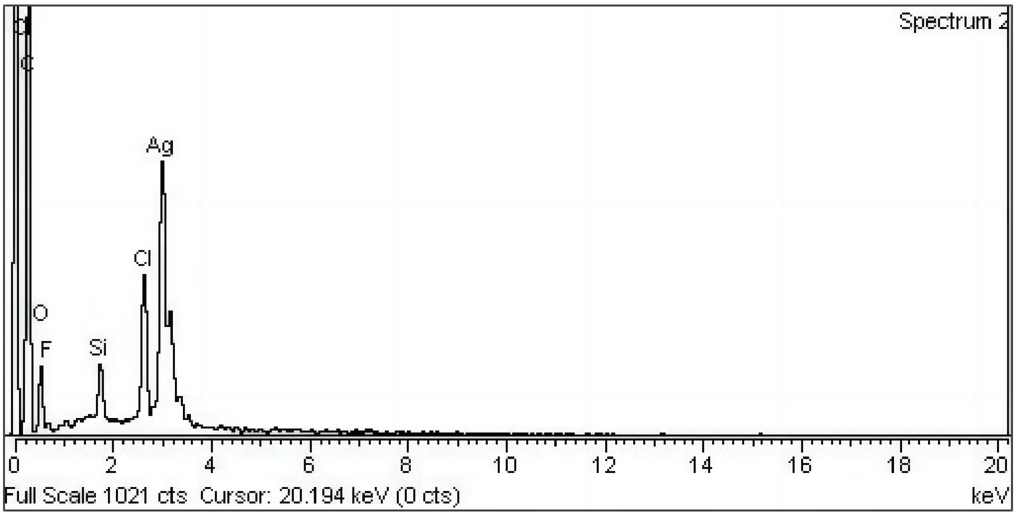

Figure 4. EDX analysis of AgNPs of *V. anthelmintica.*

3.7 Antibacterial Activity

The results of the antibacterial assay, as presented in Table 2, demonstrated that the synthesized AgNPs exhibited strong antibacterial activity against drug-resistant strains of *Staphylococcus aureus* and *Citrobacter*. In contrast, the crude plant extract of *V. anthelmintica* showed no observable antibacterial effect against either Gram-positive or Gram-negative bacteria. While plant extracts are often reported to be more effective against Gram-positive bacteria than Gram-negative ones due to differences in cell wall structure, in the case of *V. anthelmintica*, the extract did not produce any zone of inhibition [38]. Interestingly, the synthesized AgNPs followed a similar trend, showing stronger antibacterial activity against Gram-positive bacteria than against Gram-negative ones. A concentration-dependent increase in antibacterial activity was observed, with higher concentrations of AgNPs producing larger zones of inhibition. The zone of inhibition measured for *S. aureus* (Gram-positive) was 18 mm, while for *Citrobacter* (Gram-negative), it was 19 mm, indicating effective antimicrobial action, though with slightly higher efficacy against the Gram-positive strain. The antibacterial mechanism of silver nanoparticles is primarily attributed to the interaction between silver ions and the thiol groups of essential bacterial enzymes, leading to enzyme inactivation [39]. Initially, AgNPs adhere to the bacterial cell wall through electrostatic interactions, disrupting membrane integrity and cellular respiration. This interference compromises cell permeability, eventually resulting in the loss of viability and bacterial cell death [40]. The findings from this study confirm the efficacy of green-synthesized AgNPs as potent antibacterial agents. The antibacterial effects of the synthesized AgNPs were found to be comparable to those of standard antibiotics such as Vancomycin and Ciprofloxacin, as shown in Table 2. The percent inhibition was calculated in comparison to the standard antibiotics using the following formula:

% Zone of Inhibition = (Zone of inhibition of sample / Zone of inhibition of standard) × 100.

For plant extract: % Zone of inhibition = 0%

For AgNPs: % Zone of inhibition = 81.8%

These results support the potential application of green-synthesized silver nanoparticles as effective alternatives to conventional antibiotics, particularly in combating drug-resistant bacterial strains.

Table 2. Antibacterial activity of AgNPs of *V.anthemintica.*

Name of Bacteria	Zone of Inhibition (mm)		
	Extract	**AgNPs**	**Antibiotics**
S. aureus	Nil	20 ± 0.5	22 ± 0.4
Citrobacter	Nil	18 ± 0.6	19 ± 0.5

3.8 Antifungal Activity

The results of the antifungal activity assay revealed that the synthesized AgNPs exhibited good antifungal activity against Echromonium, Penicillium, and Pythium, while the methanolic plant extract of *V. anthelmintica* demonstrated moderate antifungal activity against the same fungal species. The antifungal efficacy of AgNPs increased with higher concentrations, indicating a dose-dependent response. In the control group (without any treatment), the fungal growth on a 10 cm slant in test tubes reached the full length of 10 cm for all three fungal species. When treated with the methanolic plant extract, the linear fungal growth was reduced to 9 cm for Echromonium, 8 cm for Penicillium, and 7 cm for Pythium. In contrast, the treatment with AgNPs significantly reduced the growth to 7 cm, 7 cm, and 6 cm respectively for Echromonium, Penicillium, and Pythium. This clearly indicates that AgNPs are more effective antifungal agents compared to the plant extract. Antifungal activity of the synthesized AgNPs was also found to be comparable to that of standard antifungal agents, as shown in Table 3. The percent inhibition was calculated in comparison with the positive control using the following formula:

% Inhibition = [(Linear growth in control - Linear growth in test) / Linear growth in control] × 100

Based on this calculation:

For methanolic extract:

Echromonium: [(10 - 9)/10] × 100 = 10%

Penicillium: [(10 - 8)/10] × 100 = 20%

Pythium: [(10 - 7)/10] × 100 = 30%

For AgNPs:

Echromonium: [(10 - 7)/10] × 100 = 30%

Penicillium: [(10 - 7)/10] × 100 = 30%

Pythium: [(10 - 6)/10] × 100 = 40%

These results confirm the enhanced antifungal activity of green-synthesized AgNPs over the methanolic plant extract, supporting their potential application as antifungal agents.

Table 3. Antifungal activity of AgNPs of *V.anthelmintica.*

Name of Fungal	Zone of Inhibition (cm)		
	Extract	AgNPs	Antibiotics
Echromonium	Nil	7	10
Pencillium	Nil	8	10
Pythium	Nil	9	10

3.9 Antioxident Activity

The DPPH (2,2-diphenyl-1-picrylhydrazyl) radical scavenging method was employed to evaluate the antioxidant properties of the aerial part extract of Vernonia anthelmintica. This assay is one of the most commonly used methods for assessing the antioxidant potential of plant extracts. It relies on the reduction of the stable DPPH radical, which exhibits a deep purple color with an absorption maximum at 517 nm (Table 4). When antioxidants donate a hydrogen atom or an electron to DPPH, it is converted to the reduced form (DPPH-H), resulting in a decrease in absorbance and a corresponding color change from purple to yellow. The antioxidant activity is indicative of the extract's hydrogen-donating capacity, which neutralizes the free radicals. The general scavenging reaction can be represented as:
DPPH• + (H-A) → DPPH-H + (A•)

Here, (H-A) represents the antioxidant molecule, and the degree of discoloration reflects the scavenging efficiency. The methanolic extract of *V. anthelmintica* was tested at various concentrations (10 ppm, 20 ppm, 40 ppm, 60 ppm, 80 ppm, and 100 ppm). The results demonstrated that the antioxidant activity increased with increasing extract concentration, indicating a dose-dependent response. This enhanced activity is likely due to the presence of secondary metabolites such as polyphenols and flavonoids known for their free radical scavenging capabilities (Table 4).

The DPPH radical scavenging activity was calculated using the following formula:
Inhibition (%) = [(A_control - A_test) / A_control] × 100

Where A_control is the absorbance of the DPPH solution without extract and A_test is the absorbance in the presence of the extract.

Table 4. Antioxidant activity of AgNPs of *V.anthelmintica.*

Conc ppm	Absorbance of Extract at 517 nm	Absorbance of AgNPs at 517 nm	Absorbance of Control at 517 nm	% DPPH radical scavenging of Extract	% DPPH radical scavenging of AgNPs
10	0.883	0.767	0.885	0.225	13.33
20	0.677	0.761	0.885	23.50	26.01
40	0.588	0.677	0.885	33.55	37.50
60	0.542	0.549	0.885	38.75	40.96
80	0.529	0.510	0.885	40.22	42.37
100	0.474	0.440	0.885	46.43	50.28

4. Conclusion

This study successfully demonstrated the green synthesis of AgNPs using stem and leaf extracts of *V. anthelmintica*. The biosynthesized AgNPs, with an average particle size of approximately 21 nm, were thoroughly characterized using UV-Vis spectroscopy, XRD, SEM, EDX, and Fourier-transform infrared spectroscopy (FTIR), confirming their formation, crystalline structure, elemental composition, and the functional groups responsible for their reduction and stabilization. The environmentally friendly and cost-effective synthesis approach highlights the potential of *V. anthelmintica* phytochemicals as effective reducing and capping agents. The AgNPs exhibited significant antibacterial and antifungal activity against drug-resistant microbial strains and demonstrated strong antioxidant potential. In contrast, the crude plant extracts displayed minimal or no bioactivity. These findings indicate that *V. anthelmintica*-mediated AgNPs hold great promise as candidates for the development of novel antimicrobial and antioxidant agents, supporting their potential future applications in biomedicine and sustainable nanotechnology.

Acknowledgements

The authors would like to thank the anonymous reviewers for their valuable comments and constructive suggestions, which significantly improved the quality and clarity of this paper.

Funding

This research received no specific grant from any funding agency in the public, commercial, or not-for-profit sectors.

Conflict of interest

The authors declare that they have no known competing financial interests or personal relationships that could have appeared to influence the work reported in this paper.

Generative AI statement

The authors declare that no Gen AI was used in the creation of this manuscript.

References

[1] Schaming D, Remita H. Nanotechnology: from the Ancient Time to Nowadays. Foundations of Chemistry, 2015, 17, 187-205. DOI: 10.1007/s10698-015-9235-y

[2] Shaukat S, Hassani MA, Yadgari MY, Ullah S, Iqbal MS, Khan, F, et al. Green Synthesis of Silver Nanoparticles and Its Application towards As (V) Removal from Aqueous Systems. Digest Journal of Nanomaterials and Biostructures, 2022, 17(4), 1385-1398. DOI: 10.15251/DJNB.2022.174.1385

[3] Ullah S, Shams DF, Ur Rehman, SA, Khattak SA, Noman M, Rukh G, et al. Application of Visible Light Activated Thiolated Cobalt Doped ZnO Nanoparticles towards Arsenic Removal from Aqueous Systems. Digest Journal of Nanomaterials and Biostructures, 2022, 17(2), 443-455. DOI: 10.15251/DJNB.2022.172.443

[4] Khan Y, Sadia H, Ali Shah SZ, Khan MN, Shah AA, Ullah N, et al. Classification, Synthetic, and Characterization Approaches to Nanoparticles, and Their Applications in Various Fields of Nanotechnology: A Review. Catalysts, 2022, 12(11), 1386. DOI: 10.3390/catal12111386

[5] Baig N, Kammakakam I, Falath W. Nanomaterials: A Review of Synthesis Methods, Properties, Recent Progress, and Challenges. Materials Advances, 2021, 2(6), 1821-1871. DOI: 10.1039/D0MA00807A

[6] Heiligtag FJ, Niederberger M. The Fascinating World of Nanoparticle Research. Materials Today, 2013, 16(7-8), 262-271. DOI: 10.1016/j.mattod.2013.07.004
[7] Li L, Haziq MA, Ullah S, Stanikzai AG, Bibi SD, Haq TU, et al. Remediation of Lead-contaminated Water using Green Synthesized Iron-oxide Nanoparticles: Performance and Mechanism. Air, Soil and Water Research, 2024, 17. DOI: 10.1177/11786221241278517
[8] Wang L, Hu C, Shao L. The Antimicrobial Activity of Nanoparticles: Present Situation and Prospects for the Future. International Journal of Nanomedicine, 2017, 12, 1227-1249. DOI: 10.2147/IJN.S121956
[9] Noman M, Haziq MA, Safi BU, Ullah S, Rukh G, Faiq ME, et al. Lead (II) Adsorption from Aqueous Systems using Visible Light Activated Cobalt Doped Zinc Oxide Nanoparticles. Digest Journal of Nanomaterials and Biostructures, 2022, 17(3), 839-849. DOI: 10.15251/DJNB.2022.173.839
[10] Pelaz B, Charron G, Pfeiffer C, Zhao Y, De La Fuente JM, Liang XJ, et al. Interfacing Engineered Nanoparticles with Biological Systems: Anticipating Adverse Nano-bio Interactions. Small, 2013, 9(9-10), 1573-1584. DOI: 10.1002/smll.201201229
[11] Yadgari MY, Subat S, Rashid S, Ullah S, Li L, Hassani MA, et al. Toxic Effects of Arsenic and Its Adsorption through Thiolated Cobalt Doped Silver Nanomaterials from Water Resources. Digest Journal of Nanomaterials and Biostructures, 2023, 18(4), 1339-1350. DOI: 10.15251/DJNB.2023.184.1339
[12] Yaqoob SB, Adnan R, Rameez Khan RM, Rashid, M. Gold, Silver, and Palladium Nanoparticles: A Chemical Tool for Biomedical Applications. Frontiers in Chemistry, 2020, 8, 376. DOI: 10.3389/fchem.2020.00376
[13] Bamal D, Singh A, Chaudhary G, Kumar M, Singh M, Rani N, et al. Silver Nanoparticles Biosynthesis, Characterization, Antimicrobial Activities, Applications, Cytotoxicity and Safety Issues: An Updated Review. Nanomaterials, 2021, 11(8), 2086. DOI: 10.3390/nano11082086
[14] Sharma RK, Yadav S, Dutta S, Kale HB, Warkad IR, Zbořil R, et al. Silver Nanomaterials: Synthesis and (Electro/Photo) Catalytic Applications. Chemical Society Reviews, 2021, 50(20), 11293-11380. DOI: 10.1039/D0CS00912A
[15] MubarakAli D, Kim H, Venkatesh PS, Kim JW, Lee SY. A Systemic Review on the Synthesis, Characterization, and Applications of Palladium Nanoparticles in Biomedicine. Applied Biochemistry and Biotechnology, 2023, 195, 3699-3718. DOI: 10.1007/s12010-022-03840-9
[16] Rafique M, Sadaf I, Rafique MS, Tahir MB. A Review on Green Synthesis of Silver Nanoparticles and Their Applications. Artificial Cells, Nanomedicine,and Biotechnology, 2017, 45(7), 1272-1291. DOI: 10.1080/21691401.2016.1241792
[17] Palanisamy M, Kaliyannan GV, Kumar HM. Inorganic Materials and Their Processing Techniques. Materials for Solar Energy Conversion: Materials, Methods and Applications, 2021, 189-226. DOI: 10.1002/9781119752202.ch8
[18] Kirubakaran D, Wahid JBA, Karmegam N, Jeevika R, Sellapillai L, Rajkumar M, et al. A Comprehensive Review on the Green Synthesis of Nanoparticles: Advancements in Biomedical and Environmental Applications. Biomedical Materials & Devices, 2025, 1-26. DOI: 10.1007/s44174-025-00295-4
[19] Vaseghi Z, Nematollahzadeh A, Tavakoli O. Green Methods for the Synthesis of Metal Nanoparticles using Biogenic Reducing Agents: A Review. Reviews in Chemical Engineering, 2018, 34(4), 529-559. DOI: 10.1515/revce-2017-0005
[20] Hussain I, Singh NB, Singh A, Singh H, Singh, SC. Green Synthesis of Nanoparticles and Its Potential Application. Biotechnology Letters, 2016, 38, 545-560. DOI: 10.1007/s10529-015-2026-7
[21] Jameel MS, Aziz AA, Dheyab MA. Green Synthesis: Proposed Mechanism and Factors Influencing the Synthesis of Platinum Nanoparticles. Green Processing and Synthesis, 2020, 9(1), 386-398. DOI: doi.org/10.1515/gps-2020-0041
[22] Shahzadi S, Fatima S, Shafiq Z, Janjua MRSA. A Review on Green Synthesis of Silver Nanoparticles (SNPs) Using Plant Extracts: A Multifaceted Approach in Photocatalysis, Environmental Remediation, and Biomedicine. RSC Advances, 2025, 15(5), 3858-3903. DOI: 10.1039/D4RA07519F
[23] Ohiduzzaman M, Khan MNI, Khan KA, Paul B. Biosynthesis and Characterizations of Silver Nanoparticles by Using Green Banana Peel Extract: Evaluation of Their Antibacterial and Electrical Performances. Heliyon, 2024, 10(10). DOI: 10.1016/j.heliyon.2024.e31140
[24] Dogra NK, Kumar S, Kumar D. *Vernonia anthelmintica* (L.) Willd.: An Ethnomedicinal, Phytochemical, Pharmacological and Toxicological Review. Journal of Ethnopharmacology, 2020, 256, 112777. DOI: 10.1016/j.jep.2020.112777
[25] Sharma M, Sharma M, Bithel N, Sharma M. Ethnobotany, Phytochemistry, Pharmacology and Nutritional Potential of Medicinal Plants from Asteraceae Family. Journal of Mountain Research, 2023, 17(2), 67-83. DOI: doi.org/10.51220/jmr.v17i2.7
[26] Iqbal Z, Lateef M, Jabbar A, Akhtar MS, Khan MN. Anthelmintic Activity of *Vernonia anthelmintica*. Seeds against Trichostrongylid Nematodes of Sheep. Pharmaceutical Biology, 2006, 44(8), 563-567. DOI: 10.1080/13880200600896512
[27] Githiori JB, Höglund J, Waller PJ, Baker RL. The Anthelmintic Efficacy of The Plant, *Albizia anthelmintica*, Against The Nematode Parasites Haemonchus Contortus of Sheep and Heligmosomoides Polygyrus of Mice. Veterinary Parasitology, 2003, 116(1), 23-34. DOI: 10.1016/S0304-4017(03)00218-8
[28] Kumar DG, Achar RR, Kumar JR, Amala G, Gopalakrishnan VK, Pradeep S, et al. Assessment of Antimicrobial and Anthelmintic Activity of Silver Nanoparticles Bio-synthesized from *Viscum orientale* Leaf Extract. BMC Complementary Medicine and Therapies, 2023, 23(1), 167. DOI: 10.1186/s12906-023-03982-1
[29] González AL, Noguez C Beránek J, Barnard AS. Size, Shape, Stability, and Color of Plasmonic Silver Nanoparticles. The Journal of Physical Chemistry C, 2014, 118(17), 9128-9136. DOI: doi.org/10.1021/jp5018168
[30] Nawab J, Ghani J, Ullah S, Ahmad I, Akbar Jadoon S, Ali S, et al. Influence of Agro-wastes Derived Biochar and Their Composite on Reducing the Mobility of Toxic Heavy Metals and Their Bioavailability in Industrial Contaminated Soils. International Journal of Phytoremediation, 2024, 26(11), 1824-1838. DOI: 10.1080/15226514.2024.2357640
[31] Banerjee V, Das KP. Interaction of Silver Nanoparticles With Proteins: A Characteristic Protein Concentration Dependent Profile of SPR Signal. Colloids and Surfaces B: Biointerfaces, 2013, 111, 71-79. DOI: 10.1016/j.colsurfb.2013.04.052
[32] Rao ML, Savithramma N. Biological Synthesis of Silver Nanoparticles Using Svensonia Hyderabadensis Leaf Extract and Evaluation of Their Antimicrobial Efficacy. Journal of Pharmaceutical Sciences and Research, 2011, 3(3), 1117-1121.
[33] Saikia D, Phukan P, Sakia PK. Synthesis and Characterisation of PVA Capped CdSe Nanoparticles from An Ammonia Free Bath. Internatinoal Journal of Latest Research in Science and Technology, 2014, 3(2), 156-159.

[34] Ramesh PK, Anusuya P, Kannan N, Manokari M, Revathi J, Ilavarasi V. Green Synthesis of Silver Nanoparticles Using Couroupita Guianensis Aubl. and Their Characterization. International Journal of Green and Herbal Chemistry, 2013, 2(4), 1041-1049.
[35] Rajasekar P, Priyadharshini S, Rajarajeshwari T, Shivashri C. Bio-inspired Synthesis of Silver Nanoparticles Using Andrographis Paniculata Whole Plant Extract and Their Antimicrobial Activity Overpathogenic Microbes. International Journal of Research in Biomedicine and Biotechnology, 2013, 3(3), 47-52.
[36] Gavade SM, Nikam GH, Dhabbe RS, Sabale SR, Tamhankar BV, Mulik GN. Green Synthesis of Silver Nanoparticles by Using Carambola Fruit Extract and Their Antibacterial Activity. Advances in Natural Sciences: Nanoscience and Nanotechnology, 2015, 6(4), 045015. DOI: 10.1088/2043-6262/6/4/045015
[37] Kotakadi VS, Gaddam SA, Rao YS, Prasad TNVKV, Reddy AV, Gopal DS. Biofabrication of Silver Nanoparticles Using Andrographis Paniculata. European Journal of Medicinal Chemistry, 2014, 73, 135-140. DOI: 10.1016/j.ejmech.2013.12.004
[38] McGaw LJ, Van der Merwe D, Eloff JN. In Vitro Anthelmintic, Antibacterial and Cytotoxic Effects of Extracts from Plants Used in South African Ethnoveterinary Medicine. The Veterinary Journal, 2007, 173(2), 366-372. DOI: 10.1016/j.tvjl.2005.09.004
[39] Ahmed KBA, Raman T, Veerappan A. Future Prospects of Antibacterial Metal Nanoparticles as Enzyme Inhibitor. Materials Science and Engineering: C, 2016, 68, 939-947. DOI: 10.1016/j.msec.2016.06.034
[40] Rudel T, Kepp O, Kozjak-Pavlovic V. Interactions between Bacterial Pathogens and Mitochondrial Cell Death Pathways. Nature Reviews Microbiology, 2010, 8(10), 693-705. DOI: 10.1038/nrmicro2421